Electronic Supplementary Material (ESI) for Physical Chemistry Chemical Physics.

Supporting Information

Finite pulse effects in CPMG pulse trains on paramagnetic materials

Michal Leskes and Clare P. Grey

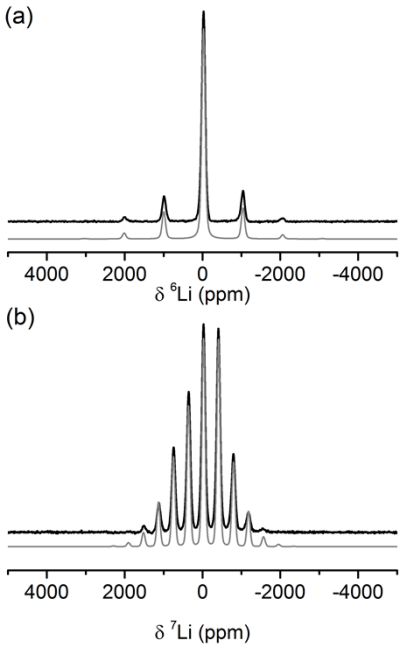

Figure S1 (a) ^{6}Li MAS spectrum of $LiFePO_4$ (black) fitted with a CSA pattern with 1280 ppm and η=0.75 (grey). (b) ^{7}Li MAS spectrum of $LiFePO_4$ (black) fitted with the same CSA values and a quadrupolar coupling constant of 60 kHz and η=1.0 (grey). Spectra were acquired on a 4.7 T spectrometer at a 30 kHz MAS frequency.

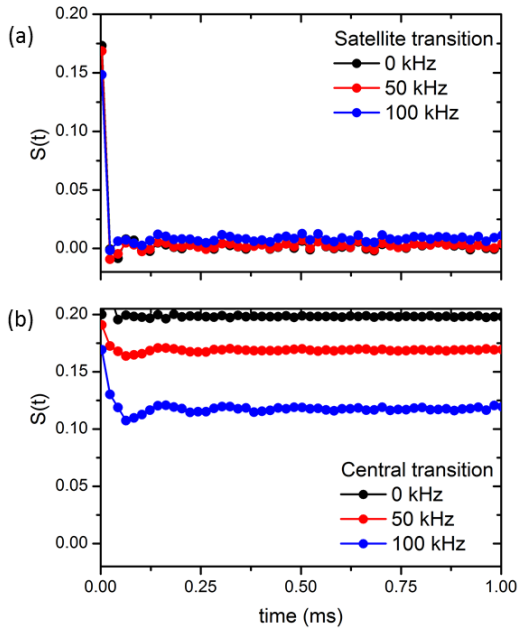

Figure S2 Simulated Hahn echo decay curves of the satellite (a) and central transitions (b) of a single ^{7}Li spin with a quadrupolar coupling of 100 kHz for varying CSA magnitude.

The effect of phase cycling and coherence pathways:

Here we will evaluate the contribution of different coherence pathways to the long T_2' constants observed with CPMG. It has been observed that off resonance effects in combination with finite pulses can result in excitation of stimulated echoes which would lead to T_1 contributions resulting in longer T_2' constants when T_1>T_2. A 16-step phase cycle was shown to reduce contribution of zero quantum coherences (and stimulated echoes) when the CPMG pulse sequence is used for sensitivity enhancement[1,2]. Results of simulated CPMG decay curves using this phase cycle are shown in Figure S3 for a system of five coupled spins. These simulated results demonstrate that even with the 16-step cycle the signal's decay rate is slower with increasing magnitude of the CSA interactions.

A similar effect is observed for a smaller system of only two coupled spins, in Figure S4. This smaller system was then used to follow the evolution of the density matrix under the effect of the CPMG pulse train. No phase cycling was used in this simulation where the various density matrix elements corresponding to zero, single and double quantum coherences (ZQ, SQ and DQ) were sampled during the echo delays in the CPMG sequence. The results, plotted in Figure S5, show that mostly SQ coherences contribute to the evolution with only small contribution of ZQ and DQ elements. Furthermore, with the addition of the CSA interaction in the simulations, the SQ coherences oscillates around a constant non-zero value indicating that indeed significant parts of the signal are effectively

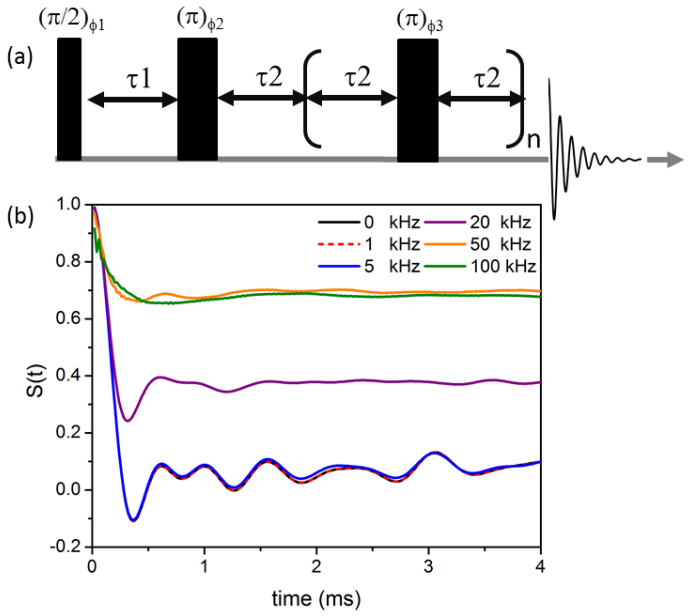

Figure S3 (a) The CPMG pulse used in simulations with a 16-step phase cycle as follows: ϕ1=x,y,-x,-y; ϕ2=y,x,y,x,-y,-x,-y,-x; ϕ3= y,x,y,x,-y,-x,-y,-x,-y,-x,-y,-x, y,x,y,x; ϕreceiver=-x,-y,x,y. The pulse lengths were τ90=1.5μs and τ180=3μs with and RF amplitude of 166.67 kHz and the echo delays were fixed at τ1=7.75μs and τ1=8.5μs. (b) The simulated decay curves for a system of 5 coupled spins (I=1/2) following the application of the CPMG sequence with 16 steps phase cycle. The first point at the top of the echo is plotted as a function of the length of CPMG train. The 5 spins coordinates are given by (R,0,0), (-R,0.0), (0,R,0), (0,-R,0) and (0,0,R) with R=3.3A and the signal intensity is plotted as a function of the CSA (equal for all spins).

"locked" (i.e. they do not evolve during the train of pulses). With no CSA the SQ coherences gradually decay to zero due to the homonuclear interactions. An enlargement of the first 100 μs, of two representative matrix elements (Figure S6) shows that in the presence of large enough CSA interactions (20 kHz in Figure S6) the SQ coherence is being continuously refocused by the 180 pulses, partially eliminating the effect of the dipolar terms which would lead to signal decay.

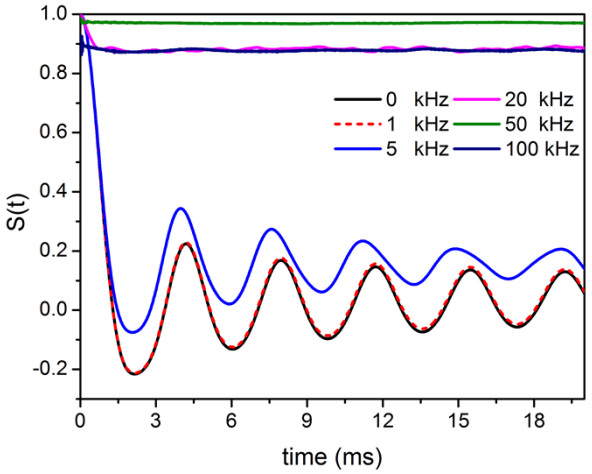

Figure S4 The simulated decay curves for a system of 2 coupled spins (I=1/2) following the application of the CPMG sequence with 16-step phase cycle. The first point at the top of the echo is plotted as a function of the length of CPMG train. The distance between the two spins was set as R=6.6A and the signal intensity is plotted as a function of the CSA (equal for both spins). The isotropic shifts for the two spins were -0.5 and 1.5 kHz.

We note that in the absence of homonuclear couplings this effect of the CSA is not observed (Figure 5 in the main text). Thus it is unlikely to be only a result of formation of stimulated echoes. Furthermore, the evolution during the cycle is mostly between SQ, DQ and ZQ (|+-><-+|) terms. The latter two coherences are formed due to the presence of the homonuclear interactions under the effect of the finite RF pulses. It is likely that for larger spin systems the homonuclear dipolar interactions can lead to contribution of additional coherences/populations and even more complicated pathways formed during the train of pulses which are difficult to remove by phase cycling due to the increasing number of pulses[3]. However, our results here from a system of five coupled spins indicate that even with a more complex network of dipolar couplings a large portion of the signal is kept in the direction of the 180 pulses and that the contribution of ZQ coherences, at least in the coupled spin systems explored in this work, do not contribute significantly to the signal's evolution.

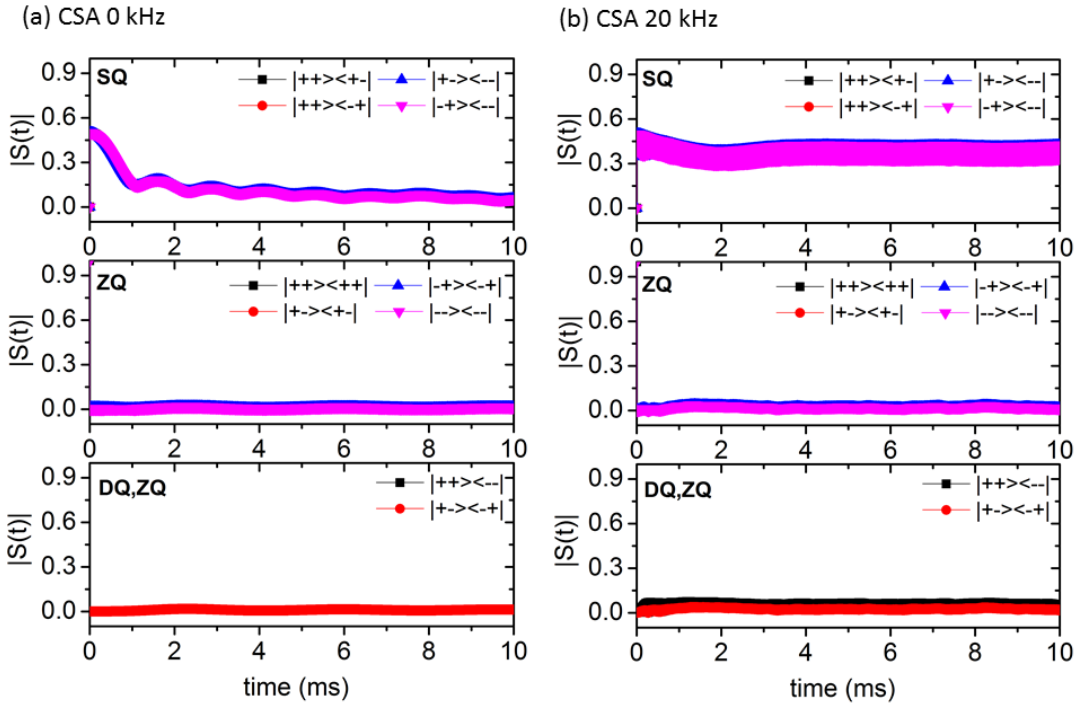

Figure S5 A simulation of the evolution of different density matrix elements of a system of two coupled spins *during* the CPMG pulse train with no phase cycle (sequence shown in Figure S6). The initial density matrix was chosen as I_z and the magnitude of various matrix elements (labelled using + as the α state and – as β state) was calculated every 0.5 μs except during the pulses. The simulation was performed without and with CSA of 20 kHz in (a) and (b) respectively. The width of the curves is due to the signal oscillations which can be seen more clearly in Figure S6.

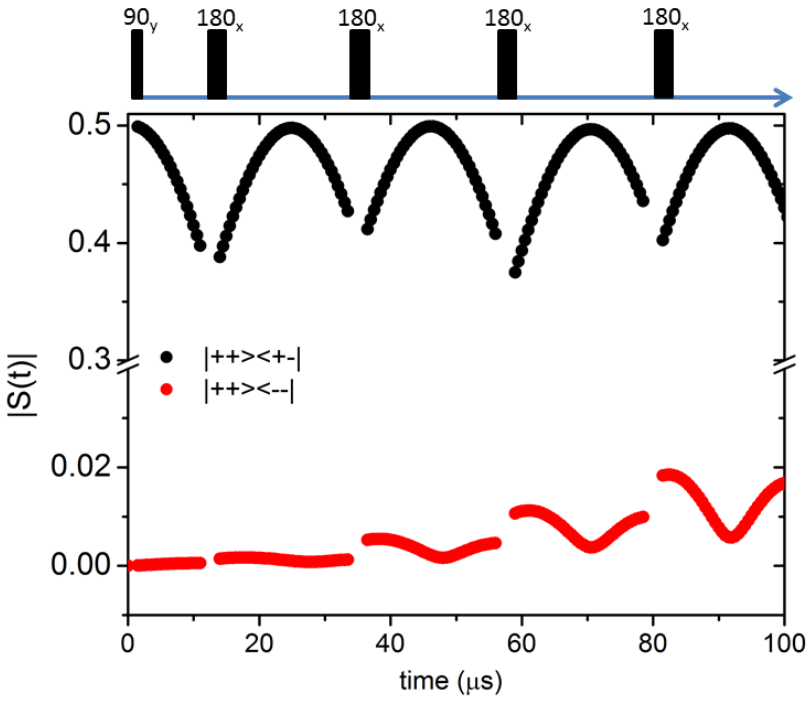

Figure S6 Enlargement of the simulated evolution of the |+ + >< - -| and |+ + >< + -| elements during the first 100 μs of the sequence (shown on the top) as in Figure S5a.

(1) Balibanu, F.; Hailu, K.; Eymael, R.; Demco, D. E.; Blümich, B. *J. Magn. Reson.* **2000**, *145*, 246–258.

(2) Franzoni, M. B.; Acosta, R. H.; Pastawski, H. M.; Levstein, P. R. *Philos. Trans. R. Soc. A Math. Phys. Eng. Sci.* **2012**, *370*, 4713–4733.

(3) Baltisberger, J. H.; Walder, B. J.; Keeler, E. G.; Kaseman, D. C.; Sanders, K. J.; Grandinetti, P. J. *J. Chem. Phys.* **2012**, *136*, 211104–211108.